**Proceedings of the ASME 2014 Dynamic Systems and Control Conference**
**DSCC2014**
**October 22-24, 2014, San Antonio, TX, USA**

# POWER SPLIT HYBRID CONFIGURATIONS FOR HUMAN-POWERED VEHICLES

**I-Ming Chen**
National Taiwan University
Taipei, Taiwan

**Chiao-Ting Li**
University of Michigan
Ann Arbor, Michigan, USA

**Huei Peng**
University of Michigan
Ann Arbor, Michigan, USA

## ABSTRACT

*This paper presents systematic analysis and design of power split-hybrid configurations using a single planetary gearset and two electric machines for human-powered vehicles. All the 12 possible power split hybrid configurations are investigated, and their performances are compared to a normal (no power assist) bicycle, and two electric bicycles. Several performance indices, including the cyclist's oxygen consumption, stamina reduction, and pedaling speed preference, are considered in the optimization problem to evaluate the bicycle designs. The dynamic programming technique is used to solve the optimization problem, and the results show that 4 of the 12 power split hybrid configurations are feasible. The optimal design, HyBike-i2, has the pedal connected to the carrier gear and one electric machine to the ring gear on the planetary gearset. The other electric machine and the driven wheel are connected to the sun gear. This design outperforms the normal bicycle and battery electric bicycles, and it achieves substantial reduction in the cyclist's stamina discharge rate and reduction in oxygen consumption when the vehicle operates in the charge-sustaining mode.*

## INTRODUCTION

Human-powered vehicles date back to ancient times and now are used for various purposes, such as urban transportation, recreation, and are frequently realized in the form of bicycles or tricycles. More recently, human-powered vehicles are seen in extreme sports, such as human-powered helicopters [1], aircrafts, or peddle boats [2, 3], and an important consideration is to push for speed and endurance of the cyclist. In developing countries, where bicycles and tricycles are still an important means for commute [4], extending cyclists' endurance is even more important as it implies longer traveling distances. In one extreme, electric bicycles are used, which can be used without any human peddling, and the common design is to add an electric motor on the crankshaft or the hub of the rear wheel [5]. The "traditional" electric bicycles often use a sizable electric motor and heavy batteries, which become deadweight when the battery is fully depleted and the human has to pedal. Their excessive weight also makes them much more difficult to be moved, e.g., carried a few steps up to reach a charging port, or lifted and transported by buses. Therefore, we are interested in exploring alternative designs that use much smaller electric machines and batteries. In this paper, we investigate the power split hybrid configuration with a planetary gearset on human-powered vehicles. In our concept, the cyclist is an integrated part of the powertrain, and his/her power output is augmented by the battery power, instead of being completely replaced. This fundamental change in design philosophy makes it possible to have a much lighter bicycle compared with traditional designs. In additional to weight reduction, the power split hybrid configuration has the potential to reduce cost. The derailleur which costs several hundred US dollars [6] can be replaced by a planetary gearset less than 30 USD [7].

Hybrid technology has been applied to a wide range of automotive applications, including automobiles [8] and off-road heavy-duty equipment [9]. Currently, the power split hybrid configuration dominates the hybrid vehicle market because it can take advantage of both series and parallel configurations to achieve better fuel economy when the power management algorithm is properly designed [10-12]. Furthermore, several studies have shown that different power split hybrid configurations should be used on vehicles with different powertrain components and power requirements [9, 13-14]. Since the powertrain characteristics of human cycling are significantly different from those of automobiles with internal combustion engines (ICEs), a different hybrid configuration may be needed for bicycles. Systematic design methodologies for on-road power split hybrid vehicles can be found in the literature [15-17]. The methodology reported in [16] is revised in this study and applied to the human-powered hybrid bicycle. Our goal is to identify the best power split hybrid configuration with smaller electric machines to ease

cyclists' efforts. Optimization problems are formulated and solved using dynamic programming to minimize the cyclist's oxygen consumption and stamina discharging while keeping the cyclist's pedaling speed (i.e. the cyclist's cadence) in the preferred range. In total, 12 split-hybrid configurations are evaluated, and their performances are compared to a normal non-hybrid bicycle and two electric bicycles.

The remainder of the paper is organized as follows: in the Modeling section, we develop models to describe the cyclist's effort to generate power and the dynamics of different bicycle configurations; the Design Methodology section presents the optimization formulation and the dynamic programming technique used to identify the optimal design; the Optimization Results section shows the comparison of the hybrid bicycle to the normal bicycle and electric bicycles; and, finally, concluding remarks are given in the Conclusion section.

## MODELING

To design a power split hybrid bicycle, we develop models for the cyclist and the bicycle transmission. The cyclist's model describes the oxygen uptake, stamina discharge, and preference in cadence during cycling. The bicycle's transmission model describes the gear connections of different configurations and their dynamics. For comparison, we also develop models for a normal (no power assist) bicycle with a 15-speed derailleur and two electric bicycles.

### The Cyclist's Model: $O_2$ uptake, stamina, and cadence preference

The oxygen uptake and heart rate have commonly been used to assess athletes' performance [18-20]. In this study, we use the oxygen uptake to measure the cyclist's effort to produce power. The oxygen consumption rate in [20] is adopted and consolidated into the static map shown in Fig. 1. The map illustrates that, when the cyclists' output power increases, the oxygen consumption also increases. This is consistent with the fact that oxygen uptake and mechanical power output is roughly linearly related [21], except for high-power cycling when a significant fraction of the power is produced anaerobically [18, 22]. In addition, the map never reaches zero because humans still consume oxygen at rest to support basal metabolism.

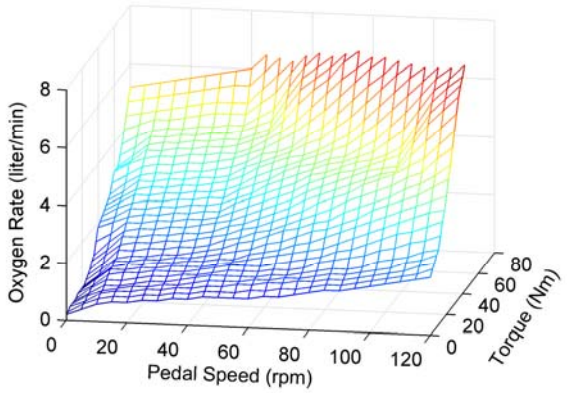


Fig. 1 Oxygen consumption rate (modified from [20])

To better understand the efficiency of the cyclist, the data in Fig. 1 is used to calculate per unit oxygen consumption, which is shown in Fig. 2. The most efficient cycling is pedaling at 70-100 rpm and 40-50 Nm, which corresponds to producing 400 watts of power. However, this power level is high and not sustainable for amateur cyclists. According to the NASA testing quoted in [23], a healthy male can maintain cycling at 200 watts for an hour, but can only last one minute at 400 watts. In other words, the oxygen uptake reflects the power generated by the cyclist, but does not reflect the exhaustion level of the cyclist. Therefore another factor, stamina consumption, must be considered.

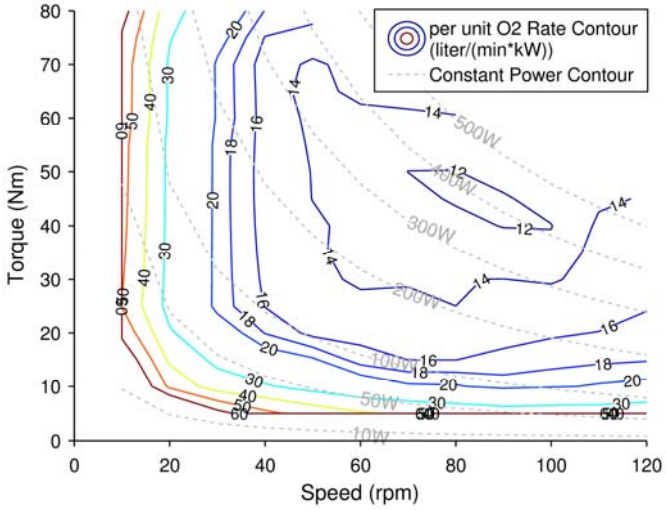


Fig. 2 Per unit oxygen consumption rate

To capture the exhaustion level of the cyclist, we adopt the time to exhaustion curve in [24]. As shown in Fig. 3, human endurance decreases drastically as the output power increases. Based on this curve, we derive an empirical formula for the stamina discharging rate, $\dot{S}$, which changes exponentially with the cyclist output power, $P_{\text{cyclist}}$, as shown in Eq. (1). This formula represents the phenomena that people are exhausted by a short burst of aggressive exercise but can endure a long low-power exercise, although the total oxygen consumption may be similar.

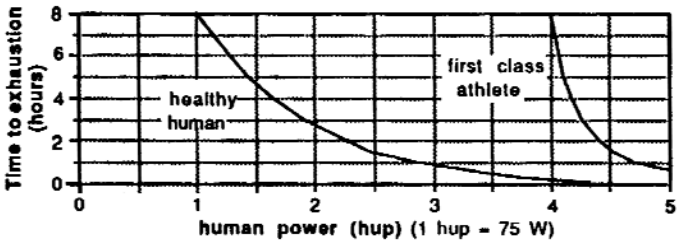


Fig. 3 Time to exhaustion for cyclist [24]

$$\dot{S} = 0.3046e^{1.493(P_{\text{cyclist}}/75)} \tag{1}$$

In addition to oxygen uptake and stamina discharge, the cyclist's cadence is another aspect to be considered for comfortable cycling. Fig. 4 shows the cycling efficiency at different cadences reported in [25], indicating that the best cycling efficiency happens when people pedal at 40-70 rpm for low-power cycling and 80-100 rpm for high-power cycling. The efficiency decreases when the cadence is outside of these ranges.

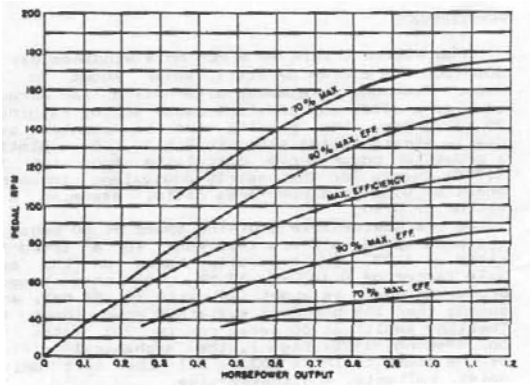


Fig. 4 Cycling efficiency at different cadences [25]

All of the three factors discussed above: the oxygen uptake, stamina discharge, and cadence, are considered in this paper to design the power split hybrid bicycle.

## Bicycle Transmission and Dynamics

Fig. 5 illustrates four different types of bicycles. The normal bicycle (abbreviated as NBike) has a 15-speed derailleur, as do the two electric bicycles (EBike-A and EBike-B). The difference between EBike-A and EBike-B is that EBike-A has an electric motor installed on the crankshaft whereas EBike-B has an electric motor on the rear hub. The power split hybrid bicycle (HyBike) is assumed to use a planetary gearset as the power split device and has two electric motors, both of which are half the size of the single motor on the EBikes. All four bicycles use chains to connect the human pedal input to the rear wheel, and the chain efficiency of the NBike and EBikes follows those reported in [26] depending on the gear ratio in use, and the HyBike is assumed to have 100% transmission efficiency due to the elimination of the derailleur.

The bicycle parameters used in this study are listed in Table 1, frontal area of the bicycle includes the cyclist and the frame.

Table 1 Bicycle Parameters

| Parameter | Value |
|---|---|
| Mass of bike and cyclist, $m$ (kg) | 100 |
| Wheel radius, $R_{\text{tire}}$ (m) | 0.33 |
| Aerodynamic drag coefficient, $C_d$ (-) [a] | 0.7 |
| Vehicle frontal area, $A_f$ (m$^2$) [a] | 0.5 |
| Rolling resistance coefficient, $C_r$ (-) | 0.015 |
| Battery Capacity, $Q$ (Wh) | 60 |

[a] Typical values for upright commuting bicycles [18]

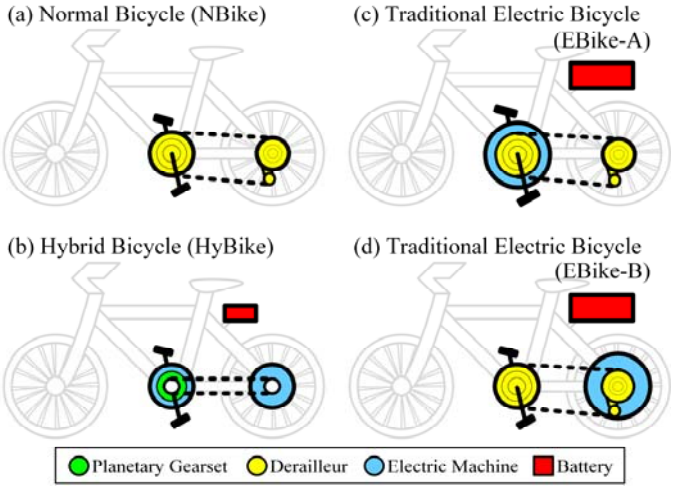


Fig. 5 Transmission sketches of HyBike, NBike, and EBike

All of the four types of bicycles require the cyclist to produce power (solely or assisted) to overcome the aerodynamic drag and rolling resistance, stated as the load torque in Eq. (2).

$$T_{\text{load}} = \left(\frac{1}{2}\rho C_d A_f v^2 + C_r mg\right)\cdot R_{\text{tire}} \tag{2}$$

where $v$ is the vehicle speed in m/s, $\rho$ is the air density in kg/m$^3$, and $g$ is the gravity constant, 9.8 m/s$^2$. The definitions of the other parameters can be found in Table 1. In a predefined riding cycle, the road load can be calculated from the vehicle speed and parameters, and then the dynamics of the NBike and two EBikes can be derived, as shown in Eqs. (3)-(5).

$$\text{For NBike: } \begin{cases} T_{\text{cyclist}} = \dfrac{T_{\text{load}}}{\gamma\cdot\eta_{\text{chain}}} \\ \omega_{\text{cyclist}} = \omega_{\text{wheel}}\cdot\gamma = \dfrac{v}{R_{\text{tire}}}\cdot\gamma \end{cases} \tag{3}$$

$$\text{For EBike-A:}\begin{cases} T_{\text{cyclist}} + T_{\text{MG}} \cdot \eta_{\text{MG}} = \dfrac{T_{\text{load}}}{\gamma \cdot \eta_{\text{chain}}} \\ \omega_{\text{cyclist}} = \omega_{\text{MG}} = \omega_{\text{wheel}} \cdot \gamma \end{cases} \quad (4)$$

$$\text{For EBike-B:}\begin{cases} T_{\text{cyclist}} = \dfrac{T_{\text{load}} + T_{\text{MG}} \cdot \eta_{\text{MG}}}{\gamma \cdot \eta_{\text{chain}}} \\ \omega_{\text{cyclist}} = \omega_{\text{wheel}} \cdot \gamma \\ \omega_{\text{MG}} = \omega_{\text{wheel}} \end{cases} \quad (5)$$

where $T_{\text{cyclist}}$ is the torque produced by the cyclist, $T_{\text{MG}}$ is the torque generated by the electric motor, $\omega_{\text{cyclist}}$ is the pedal speed, $\omega_{\text{MG}}$ is the motor speed, $\omega_{\text{wheel}}$ is the wheel speed, $\gamma$ is the gear ratio of the derailleur, $\eta_{\text{chain}}$ is the chain efficiency, and $\eta_{\text{MG}}$ is the motor efficiency.

The torque and speed relationships of the HyBike are determined based on the gear connection on the planetary gearset which, as shown in Fig. 6, typically consists of the sun gear, the ring gear, the carrier gear, and multiple pinion gears. The rotational speeds of the gears follow the relationship shown in Eq. (6), which can be visualized on the lever diagram shown on the right in Fig. 6.

$$\omega_{\text{s}} Z_{\text{s}} + \omega_{\text{r}} Z_{\text{r}} = \omega_{\text{c}} \left( Z_{\text{r}} + Z_{\text{s}} \right) \quad (6)$$

where $\omega_{\text{s}}$, $\omega_{\text{r}}$ and $\omega_{\text{c}}$ are speeds of the sun gear, ring gear and the carrier gear, and $Z_{\text{s}}$, $Z_{\text{r}}$ are the gear radii of the sun gear and ring gear.

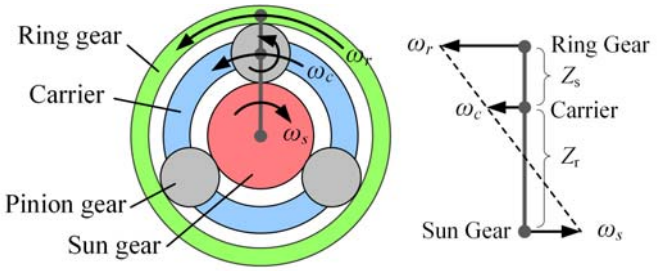


Fig. 6 Planetary gearset and the corresponding lever diagram that presents the speed relationship

There are many ways to connect the pedal, two electric machines, and the bicycle rear wheel to the planetary gearset. By applying the permutation on the lever diagram, we can find all possible power split hybrid configurations. As summarized in Table 2, there are 12 configurations: 6 input-split configurations (i1-i6) and 6 output-split configurations (o1-o6) [16]. It should be pointed out that, the i1 configuration is used in the original Toyota Prius, which has been well studied [27-29].

Table 2 The 12 Planetary Gearset Configuration for HyBike

| Configuration | Pedal | MG1 | MG2 | Wheel |
|---|---|---|---|---|
| i1 | C | S | R | R |
| i2 | C | R | S | S |
| i3 | R | C | S | S |
| i4 | R | S | C | C |
| i5 | S | C | R | R |
| i6 | S | R | C | C |
| o1 | C | S | C | R |
| o2 | C | R | C | S |
| o3 | R | C | R | S |
| o4 | R | S | R | C |
| o5 | S | C | S | R |
| o6 | S | R | S | C |

C: connected to the carrier gear; S: connected to the sun gear; R: connected to the ring gear

Depending on the configuration used, the dynamics differ. The method to automatically derive dynamic models for power split hybrid configurations can be found in [15]. As an example, Eq. (7) shows the dynamics of the i2 configuration.

$$\begin{bmatrix} mR_{\text{tire}}^2 + I_{\text{MG2}} & 0 & 0 & -Z_{\text{s}} \\ 0 & I_{\text{pedal}} & 0 & Z_{\text{r}} + Z_{\text{s}} \\ 0 & 0 & I_{\text{MG1}} & -Z_{\text{r}} \\ -Z_{\text{s}} & Z_{\text{r}} + Z_{\text{s}} & -Z_{\text{r}} & 0 \end{bmatrix} \begin{bmatrix} \dot{\omega}_{\text{s}} \\ \dot{\omega}_{\text{c}} \\ \dot{\omega}_{\text{r}} \\ F \end{bmatrix} = \begin{bmatrix} T_{\text{MG2}} - T_{\text{load}} \\ T_{\text{cyclist}} \\ T_{\text{MG1}} \\ 0 \end{bmatrix} \quad (7)$$

where $\dot{\omega}_{\text{s}}$, $\dot{\omega}_{\text{r}}$ and $\dot{\omega}_{\text{c}}$ are angular accelerations of the sun gear, ring gear and carrier gear, $F$ is the internal force acting between gears on the planetary gearset, and $I_{\text{pedal}}$, $I_{\text{MG1}}$, and $I_{\text{MG2}}$ are rotational inertia of the crankshaft and the two electric machines.

## DESIGN METHODOLOGY

Two speed profiles are used to evaluate the different bicycle designs; one is the Simple Test Cycle for feasibility verification, and the other is the Home-to-Work Commute Cycle for performance comparison. Dynamic programming is used to solve the optimization problem that considers the cyclist's oxygen uptake, stamina discharge, and cadence preference. Then, comparison is made based on the best execution of each bicycle design.

### The Optimization Problem

As reviewed in the earlier section, comfortable cycling should consider the cyclist's oxygen uptake, stamina discharge, and cadence. Therefore, a lumped objective function is used to include all these three aspects in the optimization problem when evaluating the bicycle designs. The objective function, as shown in Eq. (8), has two terms: the first term takes into

account of the three cycling aspects throughout the riding cycle, and the second term regulates the battery SOC.

$$\min J = \sum_{k=0}^{N-1} \left( f_s \cdot f_c \cdot V_{O_2} \right) \cdot \Delta k + \alpha \left( SOC_N - SOC_{\text{ref}} \right)^2 \qquad (8)$$

where $V_{O2}$ is the instantaneous oxygen consumption rate which can be found in Fig. 1, $f_s$ is the stamina factor, $f_c$ is the cadence factor, $SOC_N$ is the terminal SOC, $SOC_{\text{ref}}$ is the reference SOC level, and $\alpha$ is the weighting coefficient. Both $f_s$ and $f_c$ are determined empirically. $f_s$ is chosen to penalize high stamina discharge; however, the penalty is chosen to be weaker than exponential so that the cyclist has to pedal. $f_c$ is chosen to favor the medium cadence, and pedaling speeds lower than 40 rpm or higher than 100 rpm are penalized. To compare the Hybike and two Ebikes with NBike (which has no electric machine) fairly, we choose $\alpha$ to be large enough so that the Hybike and Ebikes operate in the charge-sustaining mode. This helps to compare the bicycle efficiency. However, in reality, battery-supported bicycles may operate in a charge-depleting manner. Depending on the bicycle type, the optimization problem has different state and control variables, and they are summarized in Table 3. The other parameters and their ranges are summarized in Table 4. In addition, the Hybike and two Ebikes are assumed to have regenerative braking.

Table 3 States & Control Variables for Optimization

| | |
|---|---|
| **NBike** | |
| **State** | Previous derailleur gear ratio |
| **Control Variable** | Current derailleur gear ratio |
| **EBike** | |
| **State** | Previous derailleur gear ratio & SOC |
| **Control Variable** | Current derailleur gear ratio & Cyclist torque |
| **HyBike** | |
| **State** | Cyclist cadence & SOC |
| **Control Variable** | Cyclist torque & MG2 torque |

Table 4 Parameter Range and Constraint

| **Parameter** | **Range** |
|---|---|
| Cyclist torque, $T_{\text{cyclist}}$ (Nm) | 0-80 |
| Cyclist cadence, $\omega_{\text{cyclist}}$ (rpm) | 0-120 |
| Motor torque, $T_{\text{MG1}}$ & $T_{\text{MG1}}$ (Nm)[a] | ±30 |
| Motor speed, $\omega_{\text{MG1}}$ & $\omega_{\text{MG2}}$ (rpm) [a] | ±200 |
| Derailleur gear ratio, $\gamma$ (-)[b] | 0.2-0.9 |

[a] Values are specific to HyBike. EBikes are assumed to have the electric machine with the same speed range, but a wider torque range, ±60 Nm.
[b] The derailleur gear ratio is discrete. The exact ratios can be found in [26].

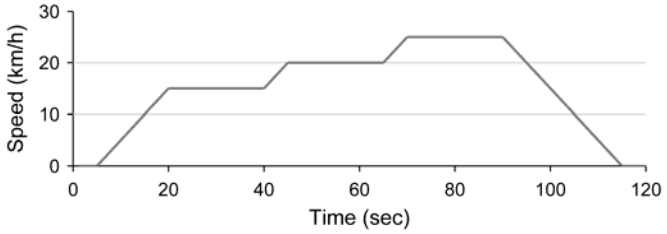

Fig. 7 The Simple Test Cycle

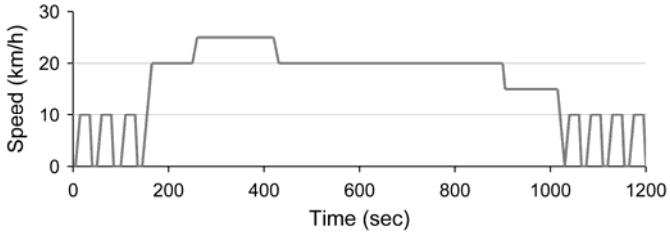

Fig. 8 The Home-to-Work Commute Cycle

### Riding Cycles

The two speed profiles used to evaluate the bicycle designs are shown in Fig. 7 and 8. The Simple Test Cycle, lasting only 120 seconds, has three representative speed levels and is used to quickly verify the feasibility of bicycle designs. After the preliminary screening, the more realistic Home-to-Work Commute Cycle is used to access the performance. The Home-to-Work Commute Cycle is 6-km long and its speed profile represents a typical bicycle commute [30], including multiple stops when traveling in a city and several segments of constant speed cruising in a suburban area.

## OPTIMIZATION RESULTS

To identify the best HyBike design, all of the 12 configurations are analyzed in the Simple Test Cycle, and dynamic programming results are used to optimize the gear ratio of the planetary gearset (the ratio of $Z_r/Z_s$, denoted as the PG ratio below). The search range of the PG ratio is from 1 to 3, although practically the PG ratio needs to be larger than 1 as the pinion gears cannot be infinitesimal. The optimization results of the Simple Test Cycle are shown in Table 5. The cyclist's oxygen uptake and stamina discharge on the NBike is used as the reference, and the performance of the other bicycle designs are normalized against the NBike. Note that, in reality, the performance improvement of the battery-supported vehicles will be greater because the charge-sustaining does not need to be enforced and more battery energy can be used to ease the riding.

Table 5 Optimization Results of the Simple Test Cycle

| **Name** | **Optimal PG ratio** | **Oxygen** | **Stamina** | **Total Cost** |
|---|---|---|---|---|
| NBike | N/A | —— The Reference Case —— | | |
| EBike-A | N/A | +0.64% | -37.9% | -4.8% |
| EBike-B | N/A | -1.91% | -39.2% | -7.9% |

| | | | | |
|---|---|---|---|---|
| HyBike-i1 | 1 | +1.42% | -53.8% | -7.0% |
| HyBike-i2 | 2.9 | -3.31% | -72.7% | -16.6% |
| HyBike-i3 | Infeasible | | | |
| HyBike-i4 | Infeasible | | | |
| HyBike-i5 | Infeasible | | | |
| HyBike-i6 | Infeasible | | | |
| HyBike-o1 | 1 | +1.26% | -49.5% | -7.0% |
| HyBike-o2 | 1.5 | +0.94% | -49.5% | -8.6% |
| HyBike-o3 | Infeasible | | | |
| HyBike-o4 | Infeasible | | | |
| HyBike-o5 | Infeasible | | | |
| HyBike-o6 | Infeasible | | | |

As shown in Table 5, only four of the 12 HyBike configurations are feasible. The HyBike-i3, i5, o3 and o5 configurations are infeasible due to the constraint violation on the cyclist's pedaling speed, and the HyBike-i4, i6, o4 and o6 configurations are infeasible due to the constraint violation on the MG1 speed. Among the four feasible HyBike designs, the HyBike-i2 configuration with the PG ratio at 2.9 is the best; it outperforms the NBike and two traditional electric bicycles. The other three HyBike configurations, i1, o1, and o2, also achieve significant reduction in stamina discharge, but the oxygen uptakes are slightly higher than NBike. Among the two traditional electric bicycles, the EBike-B is slightly better than EBike-A, because it has the electric machine on the rear hub, which avoids efficiency losses due to the chain and derailleur. However, both EBikes are less efficient than the Hybike-i2 configuration. This is because the split-hybrid configurations have the CVT (continuously variable transmission) function enabled by the planetary gearset, and thus the cyclist is more likely to pedal at a preferred speed and torque level.

Interestingly, the i2 configuration is favored over the i1 configuration; despite the fact that the latter achieves excellent performance in automotive applications (the Toyota Prius uses the i1 configuration with a PG ratio of 2.6). However, these two configurations do share some similarities. Shown in Fig. 9, both configurations have the main power source connected to the carrier gear, although the wheels are connected differently. The i2 configuration is a better design for cycling application because the preferred cyclist's pedaling speed is close to the wheel rotational speed and does not need a large gear reduction. The i2 configuration provides a more appropriate gear ratio to ease the riding by connecting the wheel to the sun gear instead of the ring gear.

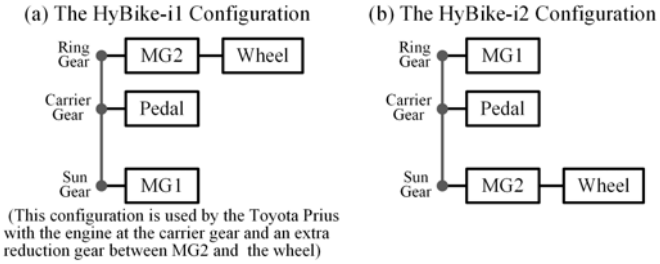


Fig. 9 Transmission sketches of HyBike-i1 and HyBike-i2

The preliminary screening in the Simple Test Cycle identifies the HyBike-i2 configuration with the PG ratio at 2.9 as the best power split hybrid design. This design is further tested in the Home-to-Work Commute Cycle. Dynamic Programming is again applied to benchmark the performance, and the cyclist efforts of the HyBike-i2 configuration and NBike are compared in Fig. 10. Since no battery support is available for NBike, the cyclist is responsible to generate the required power to overcome the road load. In particular, during the two aggressive acceleration events at 160s and 250s, the power demand is close to 300 watts. The HyBike-i2 configuration strategically utilizes the battery energy, so that the cyclist does not have to work at high power levels and the oxygen uptake and stamina discharge are both reduced. This strategic riding can be observed in Fig. 10-(c) and 10-(d). The cyclist on the HyBike-i2 pedals slightly harder to charge the battery in the first three low-speed launching events. The battery is then discharged during the two aggressive acceleration events and the high-speed cruising. The cyclist power output stays below 120 watts for most of the time and never exceeds 165 watts. Similar riding strategies are also observed on the two traditional electric bicycles (their trajectories are not shown), where the electric machine works as a motor to propel the bicycle during acceleration events, and as a generator to charge the battery at low vehicle speeds. However, the lack of the CVT feature makes the two EBikes less efficient than the HyBike-i2 configuration. The results of the Home-to-Work Commute Cycle are summarized in Table 6.

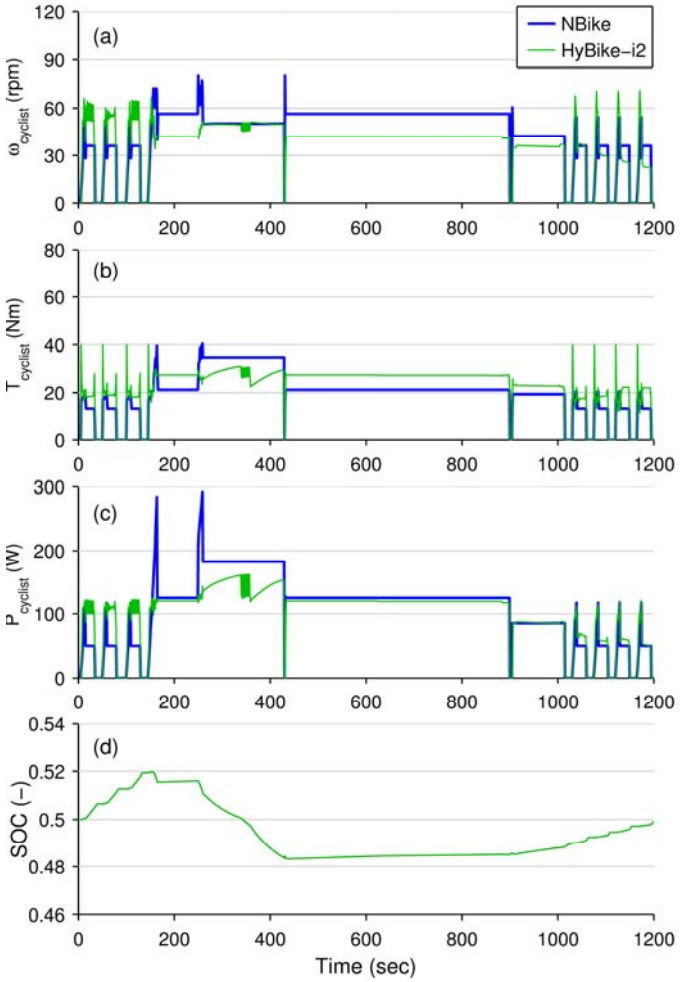


Fig. 10 Cyclist efforts and SOC trajectory in the Home-to-Work Commute Cycle

Table 6 Optimization Results of the Home-to-Work Cycle

| Name | Oxygen | Stamina | Total Cost |
|---|---|---|---|
| NBike | —— The Reference Case —— | | |
| EBike-A | -1.33% | -25.5% | -6.7% |
| EBike-B | -2.45% | -27.5% | -9.0% |
| Hybike-i2 (PG ratio = 2.9) | -3.26% | -34.0% | -13.0% |

Fig. 11 shows how differently the cyclist has to work on the NBike and HyBike-i2 in the Home-to-Work Commute Cycle. The cyclist on the NBike has to work at higher power levels for noticeable amounts of time, whereas the cyclist on HyBike-i2 works consistently at lower power levels. This explains why the HyBike-i2 configuration (and the other battery-supported vehicles) is able to significantly reduce the stamina discharge. As stated earlier, the stamina discharge is exponential to the cyclists' power output; therefore, keeping the cyclist working at a medium and constant power level is very effective to reduce the stamina discharge. In addition, Fig. 11 also shows that HyBike-i2 not only keeps the cyclist's power output low, but also allows the cyclist to ride within the preferred cadence range.

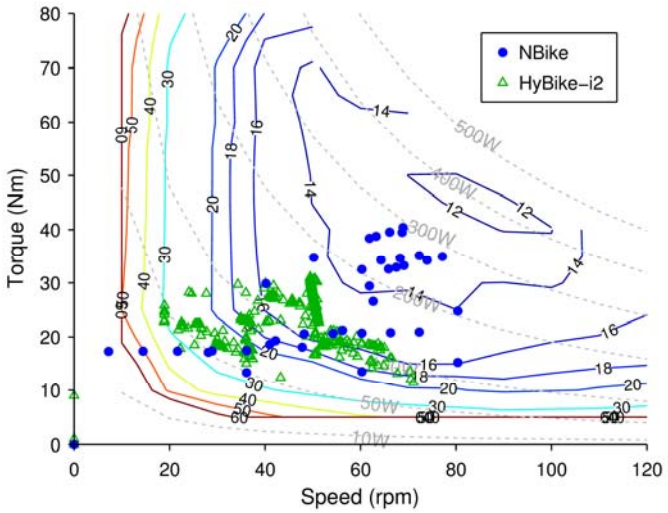


Fig. 11 Operation of the cyclist in the Home-to-Work Commute Cycle

In this study, we focus on analyzing the efficiency of the bicycle transmission and do not explicitly address the battery sizing. All bicycle designs are assumed to have a 60 Wh battery and operate in the charge-sustaining mode. However, based on the greater reduction in stamina discharge HyBike-i2 achieves, it is highly possible that HyBike-i2 can use a smaller battery than traditional electric bicycles while providing equivalent riding assist to the cyclist.

## CONCLUSION

The design of a power split hybrid human-powered vehicle is presented in this paper. The planetary gearset is used as the power-split device, and 12 configurations are investigated. Three cycling performance factors, the cyclist's oxygen uptake, stamina discharge, and cadence preference, are considered in the optimization problem when evaluating the performance of the bike designs. Dynamic programming is used to benchmark the performance of the 12 configurations and optimize the gear ratio of the planetary gearset (the PG ratio). Then, these 12 configurations are compared to a normal (no power assist) bicycle and two traditional electric bicycles. The results show that 4 of the 12 configurations are feasible, and the optimal design is the HyBike-i2 configuration (shown in Fig. 9-(b)) with the PG ratio at 2.9. The HyBike-i2 configuration outperforms the normal bicycle and traditional electric bicycles because of the CVT feature enabled by the planetary gearset. In

addition, it achieves substantial reduction in the cyclist's stamina discharge and some reduction in oxygen uptake in the charge-sustaining mode. The performance improvement is greater in the charge-depletion mode.

It is worth mentioning that the winning design, the HyBike-i2 configuration, is different from the power split hybrid configuration used in hybrid electric passenger cars. This is because the characteristics of human cycling are different from internal combustion engines. The main differences include:

1) Human cyclists can "get tired" but machines do not. Unlike on-road hybrid vehicles aiming to regulate the engine operation within the "sweat spot" for better per unit fuel consumption, the HyBike-i2 configuration regulates the cyclist's power output to prevent stamina depletion.

2) The cyclist cadence is relatively close to the wheel speed and does not need a large gear reduction like most ICE automobiles do.

These human-specific characteristics require a transmission design different from those used for automobiles. The implication is that different transportation electrified applications may use different power split configurations that suit their specific operations. The modeling technique and design methodology developed in this paper can be applied to other applications.

In the future, to further understand the characteristics of the hybrid human-powered vehicle, a more representative riding cycle including speed and grade profile will be defined since the road grade can significantly affect the cyclist's riding experience. Effect of different cycles and different SOC strategies will be discussed. And a real-time control strategy will be proposed based on the optimization results for practical implementation.

## REFERENCES


[1] The Atlas Human-Powered Helicopter, [online] 2014. http://www.aerovelo.com/ (Accessed: 1/17/2014).

[2] International Human Powered Vehicle Association. IHPVA Events, [online] 2010. http://www.ihpva.org/events.htm (Accessed: 2/24/2014).

[3] World Human Powered Speed Challenge, [online] 2013. http://www.wisil.recumbents.com/wisil/whpsc2013/speedchallenge.htm (Accessed: 2/24/2014).

[4] J. Weinert, J. Ogden, D. Sperling and A. Burke, "The future of electric two-wheelers and electric vehicles in China," *Energy Policy,* vol. 36, pp. 2544-2555, 2008.

[5] Electric Bicycle Reviews, [online] 2013. http://www.electricbicyclereviews.com/ (Accessed: 2/24/2014).

[6] Performance Bicycle, [online] 2014. http://www.performancebike.com/ (Accessed: 3/11/2014).

[7] KHK Kohara Gear Industry Co., Ltd., [online] 2014. http://www.khkgears.co.jp/en/ (Accessed: 3/11/2014).

[8] Alternative Fuels and Advanced Vehicles Data Center. Data, Analysis, and Trends: Vehicle—HEV Sales by Model, [online] 2010. http://www.afdc.energy.gov/afdc/data/vehicles.html (Accessed: 6/14/2012).

[9] S. Baseley, C. Ehret, E. Greif and M. G. Kliffken, "Hydraulic hybrid systems for commercial vehicles," *SAE Paper,* 2007-01-1455, 2007.

[10] B. Conlon, "Comparative analysis of single and combined hybrid electrically variable transmission operating modes," *SAE Paper,* 2005-01-1162, 2005.

[11] T. Grewe, B. Conlon and A. Holmes, "Defining the general motors 2-mode hybrid transmission," *SAE Paper,* 2007-01-0273, 2007.

[12] C.-C. Lin, H. Peng, J. Grizzle and J.-M. Kang, "Power management strategy for a parallel hybrid electric truck," *IEEE Transactions on Control Systems Technology,* vol. 11, pp. 839-849, 2003.

[13] C.-T. Li and H. Peng, "Optimal configuration design for hydraulic split hybrid vehicles," in *American Control Conference*, Baltimore, MD, 2010, pp. 5812-5817.

[14] X. Zhang, C.-T. Li, D. Kum and H. Peng, "Prius+ and Volt-: configuration analysis of power-split hybrid vehicles with a single planetary gear," *IEEE Transactions on Vehicular Technology,* vol. 61, pp. 3544-3552, 2012.

[15] J. Liu and H. Peng, "A systematic design approach for two planetary gear split hybrid vehicles," *Vehicle System Dynamics,* vol. 48, pp. 1395-1412, 2010.

[16] C.-T. Li, X. Zhang and H. Peng, "Design of power-split hybrid vehicles with a single planetary gear," in *Dynamic System and Control Conference*, Fort Lauderdale, FL, 2012, pp. 1347-1355.

[17] K. Cheong, P. Li and T. Chase, "Optimal design of power-split transmission for hydraulic hybrid passenger vehicles," in *American Control Conference*, San Francisco, CA, 2011, pp. 3295-3300.

[18] D. G. Wilson, *Bicycling Science*, 3rd ed. Cambridge, MA: MIT Press, 2004.

[19] E. W. Banister and R. C. Jackson, "The effect of speed and load changes on oxygen intake for equivalent power outputs during bicycle ergometry," *Internationale Zeitschrift für angewandte Physiologie Einschließlich Arbeitsphysiologie,* vol. 24, pp. 284-290, 1967/12/01 1967.

[20] J. R. Coast and H. G. Welch, "Linear increase in optimal pedal rate with increased power output in cycle ergometry," *European Journal of Applied Physiology,* vol. 4, pp. 339-342, 1985.

[21] M. Reger, J. E. Peterman, R. Kram and W. C. Byrnes, "Exercise efficiency of low power output cycling," *Scandinavian Journal of Medicine & Science in Sports,* vol. 23, pp. 713-721, 2013.

[22] S. R. Bussolari and E. R. Nadel, "The physiological limits of long-duration human power production--lessons learned

from the Daedalus project," *The Technical Journal of the IHPVA,* vol. 7, pp. 8-10, 1985.
[23] D. G. Wilson, "HPV science," *The Technical Journal of the IHPVA,* vol. 24, pp. 4-14, 2003.
[24] D. J. Malewicki, "New unified performance graphs and comparisons for streamlined human powered vehicles," in *2nd HPV Scientific Symposium*, 1983.
[25] F. DeLong, *DeLong's Guide to Bicycles and Bicycling*. Radnor, PA: Chilton, 1978.
[26] C. R. Kyle and F. Berto, "The mechanical efficiency of bicycle derailleur and hub-gear transmissions," *The Technical Journal of the IHPVA,* vol. 52, pp. 3-11, 2001.
[27] C. Mansour and D. Clodic, "Dynamic modeling of the electro-mechanical configuration of the Toyota Hybrid System series/parallel power train," *International Journal of Automotive Technology,* vol. 13, pp. 143-166, 2012.
[28] J. Liu and H. Peng, "Modeling and control of a power-split hybrid vehicle," *IEEE Transactions on Control Systems Technology,* vol. 16, pp. 1242-1251, 2008.
[29] N. Kim, A. Rousseau and E. Rask, "Vehicle-level control analysis of 2010 Toyota Prius based on test data," *Journal of Automobile Engineering,* vol. 226, pp. 1483-1494, 2012.
[30] J. Paefgen and F. Michahelles, "Inferring usage characteristics of electric bicycles from position information," in *the 3rd International Workshop on Location and the Web*, Tokyo, Japan, 2010, pp. 1-4.